EDDY CURRENT EFFECT IN A MAGNETIC BEARING MODEL

Takeshi Yoshimoto

ABSTRACT

Eddy current problem in a simple magnetic bearing model is treated. Such a problem is very important in the case when solid steel is used as a shaft material. We have made the calculation about eddy current effect on a hypothetical, simplified model by finite element method.

Diagrams of flux distribution in both the air-gap and the shaft material are obtained at various rotor speeds. We can clearly see how eddy current induced in a shaft affects main flux of electromagnets. The form of current distribution for producing main flux of electromagnets is taken as both sinusoidal and rectangular. We have also calculated the characteristics of attractive force and counter torque vs. rotor speed.

This model is suitable for examining effects of various parameters. No suspicious rugged aspects were perceived in our calculation results. This confirms that our way of making subdivision is good. Our results make it possible to predict the realistic performance tendency and to know the working region less affected by eddy current.

FINITE ELEMENT ANALYSIS

Model

Fig.1 is basic diagram of a magnetic bearing. Four electromagnets are usually used to suspend the rotating shaft. Our subject is now restricted to considering how eddy current induced in a shaft affects the main flux of electromagnets. For this purpose, we derived a hypothetical, simplified model such as shown in Fig.2, in which 8 poles in Fig.1 are transformed into 4 poles and current density for magnetizing 4 poles is distributed in a form sinusoidal around the inner surface of the stator. We also deal with rectangular form distribution of current density, afterwards.

Finite element analysis has been performed under the following assumptions:

(1) The field is two dimensional.
(2) The model has 4 poles with the same magnetic force.
(3) Gap length is uniform around the shaft.
(4) Current is given as a sheet, and therefore there are no slots for current bars.
(5) Current distribution around the inner circumference of the stator is either sinusoidal or rectangular.
(6) It is assumed that the shaft is standing still, while the poles of electromagnets are rotating.
(7) Relative permeability of the shaft is taken as 100, and its conductivity is taken as a parameter.
(8) Magnetic saturation and hysteresis of shaft material is neglected.

Formulation

As for the distribution form of magnetizing current density, we deal with 2 types, one sinusoidal and the other rectangular. In the case of rectangular distribution, we expand it into Fourier series and calculate vector potentials for each harmonics and finally synthesize each vector potentials at every node. After all, it is concluded that calculation under sinusoidally distributed current density is basic.

Manuscript received March 7, 1983.

Takeshi Yoshimoto is with the Department of Electrical Engineering, Ishikawa Technical College, Tsubata, Ishikawa-pref. 929-03 JAPAN

Next we show finite element method of formulation for the case with sinusoidal current distribution.

From Maxwell's field equations, we get equation (1). [1]

$$\frac{1}{\mu}\mathrm{rot}\cdot\mathrm{rot}\,\boldsymbol{A} = \boldsymbol{J} - \sigma\frac{\partial \boldsymbol{A}}{\partial t} \qquad (1)$$

If $\boldsymbol{J}$ is supposed to be a vector with rotational frequency ω such as $\boldsymbol{J}=\bar{J}\exp(j\omega t)$, $\boldsymbol{A}$ will also be a sinusoidally changing vector such as $\boldsymbol{A}=\bar{A}\exp(j\omega t)$. Then equation (1) can be re-written as follows.

$$\frac{1}{\mu}\mathrm{rot}\cdot\mathrm{rot}\,\bar{A} = \bar{J} - j\omega\sigma\bar{A} \qquad (2)$$

In this case, we can have following well known energy functional shown in equation (3). [2],[3]

$$F = \int\left[\left(\frac{\bar{B}}{2\mu}\right)^2 - \bar{J}\bar{A} + j\omega\frac{1}{2}\sigma\bar{A}^2\right]dv \qquad (3)$$

Both $\bar{J}$ and $\bar{A}$ have only z-component. Real current density distribution is shown as,

$$J = J_m\cos\left(\frac{\pi}{\tau}(vt+l)\right)$$

$$= J_m\cos(\omega t + p\theta) \qquad (4)$$

Expressing it in a complex form,

$$\bar{J}\exp(j\omega t) = J_m\exp(j(\omega t+p\theta)) \qquad (5)$$

$$\bar{J} = J_m(\cos p\theta + j\sin p\theta) \qquad (6)$$

where, v :circumferential relative velocity
τ :pole pitch
p :number of pole-pairs
ω :rotational angular frequency $2\pi p\cdot\left(\frac{\mathrm{REV}}{60}\right)$
θ :electrical phase from x-axis
l :circumferential distance from x-axis

By using this current expression, we can carry out FEM formulation shown in many references such as [2],[3], [4]. Finally we get the following complex coefficient simultaneous equations (7).

$$\left[[R_e] + j\cdot[I_m]\right]\cdot[A] = \left[J_m\cos p\theta + j\cdot J_m\sin p\theta\right] \qquad (7)$$

The matrices $[R_e]$ and $[I_m]$ are determined by the geometries and material properties. We have solved equation (7) by Gauss elimination method.

Computation by superposition law

Eddy current problems must be solved in at least 1 pole-pair region.[5] Also, because of complex type equations, about twice the memory used in ordinary ones are needed. To make it more difficult, inspection of eq.(6) shows there are no periodic boundaries. In other words, cosine term and sine term do not have any common symmetrical axes, as can be seen in Fig.3.

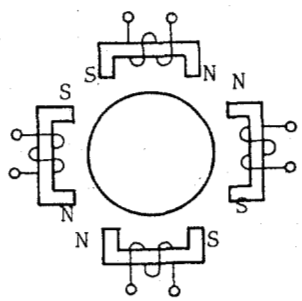

Fig.1 Basic Diagram of a Magnetic Bearing

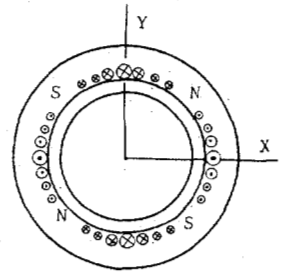

Fig.2 Hypothetical, Simplified Model

But computation for whole region would not be practical from the view point of memory, computation time and accumulated errors.

We have managed to overcome these difficulties by using law of superposition. It leads to two separate computations for $J_m \cos p\theta$, and for $J_m \sin p\theta$, each of which has periodic boundaries. The solution for region A-E for $J_m \cos p\theta$ is found to correspond with the solution for region B-F for $J_m \sin p\theta$.

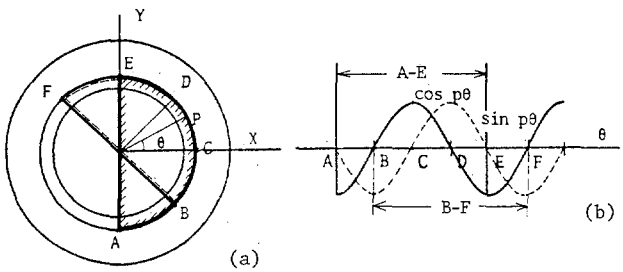

Fig.3 Current Distribution and Periodic Boundaries

We have only to get vector potentials AP(I) for $J_m \cos p\theta$. The following equation makes it possible to get the final vector potentials VP(I).

$$VP(I)=AP(I)+j\cdot AP(I+IAD) \quad (I=1,2,\cdots,3IAD) \tag{8}$$

where, IAD is number of nodes for 1/2 pole pitch.

Rectangular form current distribution

In this case we expand this wave form into Fourier series up to 29 th harmonic. Nth harmonic amplitude is shown in the following equation.

$$AMPLI(N)=\frac{4}{\pi N} I_d \cdot \sin\left(\frac{N\cdot\pi\cdot RATIO}{2}\right) \tag{9}$$

where, $RATIO = \frac{DEG}{180}\cdot p$

I_d : amplitude

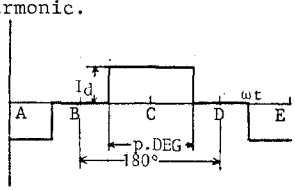

Fig.4 Rectangular Current Density

Vector potentials are obtained for each harmonics, in the way shown above. For Nth harmonic, mesh is shrunk to have 1/N angle of the mesh diagram for the fundamental wave. Vector potentials for each harmonics are finally synthesized for each node. When RATIO(or DEG) is specified, amplitude I_d is changed so as to have same ampere turns as in the sinusoidal excitation.

$$I_d = J_m / (DEG\cdot\pi/180) \tag{10}$$

FLUX DISTRIBUTION

Fig.5 shows flux density in the air-gap, distributed over one and a half pole pitch, (a) for sinusoidal, (b) for rectangular (RATIO=2/3, DEG=60°), (c) for rectangular (RATIO=1/6, DEG=15°). In each case, it is observed that flux density is gradually skewed and demagnetized as the rotor speed increases. It is what we call eddy current effect.

Fig.6 shows equi-potential diagrams for RATIO=1/6 rectangular excitation, (a) N=10 rpm, (b) N=100 rpm, (c) N=400 rpm. This time we can observe eddy current effect in the whole. In proportion as the rotating speed increases, it is recognized that the flux lines are skewed towards revolving direction and concentrated towards surface of a steel shaft at the same time. The thick line shows zero potential line.

ATTRACTIVE FORCE AND COUNTER TORQUE

Attractive force per pole is calculated by integrating radial magnetic force density around the shaft surface. Counter torque is also calculated by integrating electro-magnetic force torque density around the inner surface of the stator. [6]

Their characteristics for the sinusoidal excitation case are shown in Fig.7 and Fig.8, where gap length is taken as a parameter. In both figures, the rotor speed multiplied by conductivity is taken as x-axis variable. Both attractive force and counter torque is normalized by the square of the maximum current density. Attractive force starts to decrease by eddy current effect beyond a certain rotor speed. It is confirmed that when a low conductivity material is used, the fall-down of attractive force delays, because of reduction of eddy current. As the eddy current increases, the main flux is skewed gradually by its cross-magnetizing effect.
This is what causes the increase of counter torque in Fig.8. Beyond a certain rotor speed, counter torque starts to decrease owing to the demagnetizing effect of eddy current.

In the case when current distribution is of rectangular form, characteristics of attractive force and counter torque per pole versus rotor speed are similar to those in the sinusoidal excitation.
In the case above DEG=60°, fundamental component, which is dominant over all other harmonics, governs two characteristics. In the case below DEG=30°, components of harmonics which become to be comparable with fundamental's, affect two characteristics.

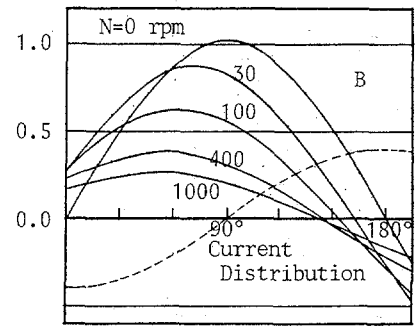

Fig.5 Air-gap Flux Density Distribution (gap=1.2 mm)

(a) for sinusoidal excitation case

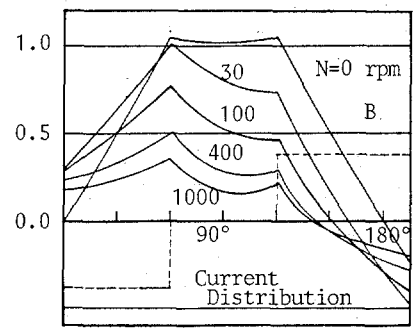

(b) for DEG=60° rectangular excitation case

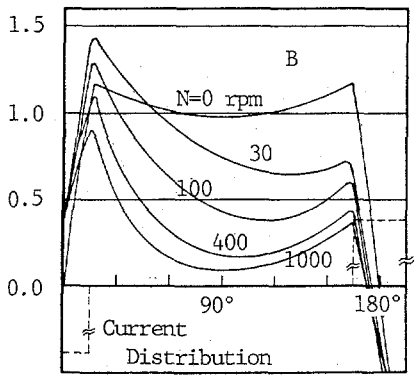

(c) for DEG=15° rectangular excitation case

In Fig.9, we show the ratio of counter torque to attrctive force. The upper and the lower lines are the ratios, respectively for sinusoidal excitation and for DEG=15° rectangular form excitation. When DEG varies from 15° to 90°, the corresponding ratio enters the range between the two lines.

CONCLUSION

The effect of eddy current induced in a shaft of a magnetic bearing model were calculated under the condition of constant permeability by finite element method. By obtaining flux distribution in the air-gap and the rotating shaft, we have clarified demagnetizing effect and cross-magnetizing effect of eddy current. Also we obtained the characteristics of attractive force and counter torque per pole vs. rotor speed. Though magnetic saturation of a shaft material must be considered hereafter, our results make it possible to predict the realistic performance tendency and also to know the working region which is less affected by eddy current. Consideration as to the end effect and measuring in an experimental model are also the problems we must carry out from now.

REFERENCES

[1] S.Takeyama,Electromagnetic Field Phenomena, Tokyo, Maruzen Co.ltd, 1969.

[2] M.V.K.Chari, "Finite Element Solution of the Eddy Current Problem in Magnetic Structures," IEEE Trans. Power and App. Syst., vol PAS-93,Jan./Feb. 1974

[3] J.R.Brauer, "Finite Element Analysis of Electromagnetic Induction in Transformers," Text A pap. IEEE Power Eng.Soc. 1977 Winter A-77122-5.

[4] O.W.Andersen, "Transformer Leakage Flux Program Based on the Finite Element Method," IEEE Trans. Power and App. Syst.,vol PAS-92,Mar./Apr.1973.

[5] T.Nakata and N.Takahashi, Proceedings of Symposium for FEM Application to Electrical and Electronic Engineering,p49, Society for Simulation Techniques, Dec.1979.

[6] M.Ito, N.Fujimoto,et al., "Effects of Broken Rotor Bar on Unbalanced Magnetic Pull and Torque in Induction Motors," Trans. of JIEE,vol 100-B,1980.

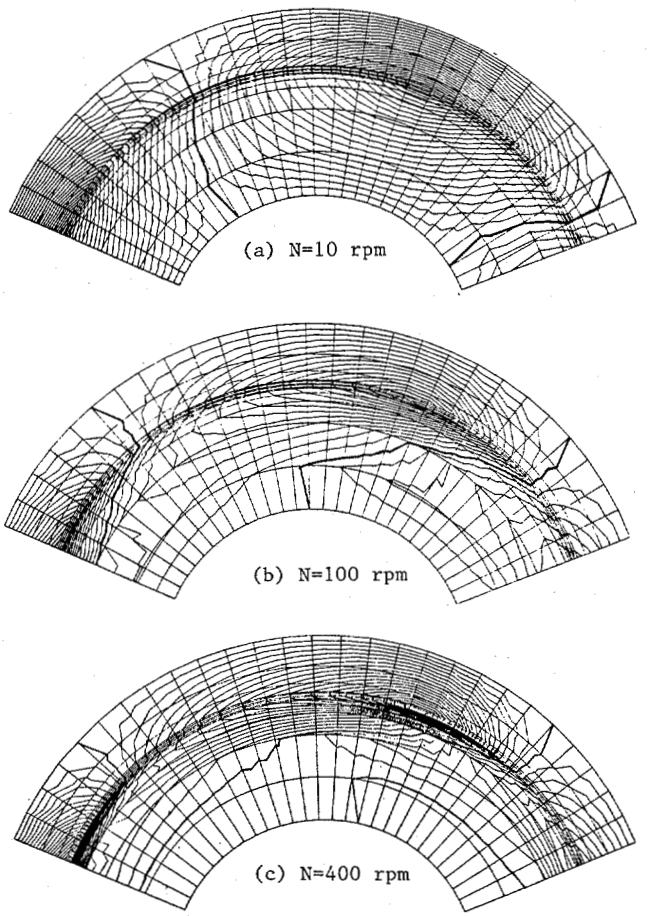

Fig.6 Equi-potential Diagrams for DEG=15° Rectangular Excitation Case (σ=1.0x10^7, gap=1.2 mm)

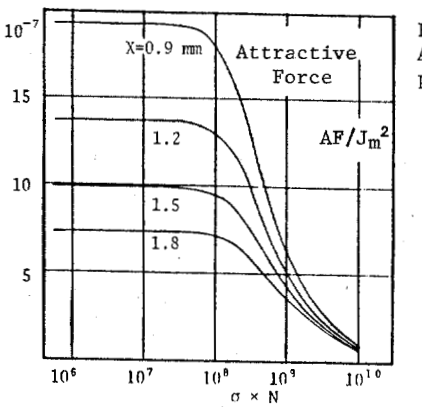

Fig.7 Attractive Force per Pole Kg/(A/m)^2

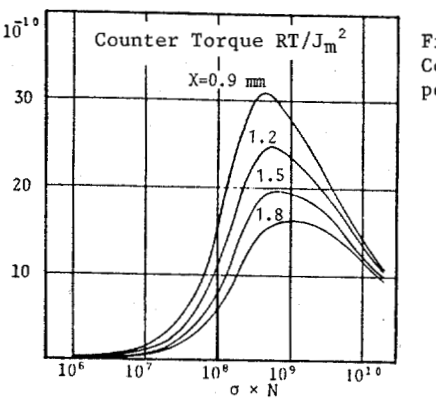

Fig.8 Counter Torque per Pole Kgm/(A/m)^2

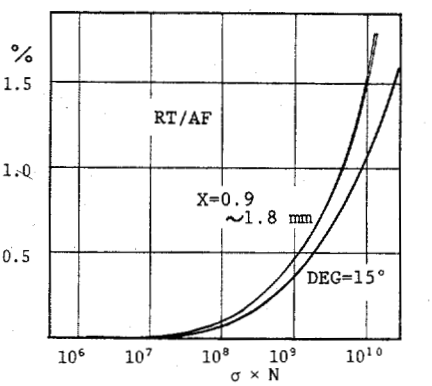

Fig.9 Ratio of Counter Torque to Attractive Force